Nuclear Equation of State from Observations of Short Gamma-Ray Burst Remnants

Paul D. Lasky,* Brynmor Haskell, and Vikram Ravi†
School of Physics, University of Melbourne, Parkville, VIC 3010, Australia

Eric J. Howell and David M. Coward
School of Physics, University of Western Australia, Crawley WA 6009, Australia

The favoured progenitor model for short γ-ray bursts (SGRBs) is the merger of two neutron stars that triggers an explosion with a burst of collimated γ-rays. Following the initial prompt emission, some SGRBs exhibit a plateau phase in their X-ray light curves that indicates additional energy injection from a central engine, believed to be a rapidly rotating, highly magnetised neutron star. The collapse of this 'protomagnetar' to a black hole is likely to be responsible for a steep decay in X-ray flux observed at the end of the plateau. In this letter, we show that these observations can be used to effectively constrain the equation of state of dense matter. In particular, we show that the known distribution of masses in binary neutron star systems, together with fits to the X-ray light curves, provide constraints that exclude the softest and stiffest plausible equations of state. We further illustrate how a future gravitational wave observation with Advanced LIGO/Virgo can place tight constraints on the equation of state, by adding into the picture a measurement of the chirp mass of the SGRB progenitor.

PACS numbers: 26.60.-c, 97.60.Jd, 04.30.Tv

Recent observations of long and short γ-ray bursts (SGRBs) show plateau phases in the X-ray light curves that last hundreds of seconds [1–6] and provide evidence for ongoing energy injection through a central engine [2, 7, 8]. The main candidate for the central engine in SGRBs is a rapidly rotating, highly magnetised neutron star (NS) [9–12] that forms following the coalescence of two NSs [13–19]. Recent analytic fits to X-ray light curves supports this 'protomagnetar' interpretation of a central engine for both long [20–23] and short GRBs [4–6]. Excitingly, some objects exhibit an abrupt cut-off in the X-ray flux $\sim 100\,$s after the initial trigger [5, 20, 21]. This has been interpreted as the metastable protomagnetar collapsing to form a black hole.

From a theoretical perspective, the coalescence of binary NSs can follow a number of evolutionary paths. If the merger remnant is sufficiently massive, it immediately collapses to a black hole, or forms a dynamically unstable hypermassive NS that is supported by strong differential rotation and thermal pressure [18, 24]. Magnetic braking terminates differential rotation on the Alfvén timescale [25, 26] implying that the object collapses in ~ 10–$100\,$ms. If the merger remnant is less massive it forms a supramassive, metastable protomagnetar [27, 28] in which centrifugal forces from uniform rotation support a higher mass than the non-rotating Tolman-Oppenheimer-Volkoff (TOV) maximum mass [29]. Such a supramassive star spins down until the centrifugal force is insufficient to support the mass, at which point it collapses to a black hole. The recent discovery of $\sim 2\,M_\odot$ NSs [30, 31] demonstrates that the equation of state (EOS) permits massive enough NSs for supramassive stars to be created from the merger of two NSs [32]. Finally, a merger remnant that is less massive than the TOV maximum mass will survive as a stable NS.

In this letter, we focus on the possibility that protomagnetars drive the plateau phases of SGRB X-ray light curves. The loss of rotational energy from the NS powers the emission, and a simple spin-down model can be fit to the light curve to obtain the initial spin period, p_0, and surface dipolar magnetic field, B_p, of the protomagnetar [4, 5, 11]. When an abrupt decay in X-ray luminosity is also observed, this is interpreted as the star having spun down to the point at which centrifugal forces can no longer support its mass against gravity [20, 21]. The time between the initial prompt emission and the decay, $t_{\rm col}$, is hence interpreted as the collapse time of the protomagnetar. Given p_0 and B_p, the time it takes the NS to collapse will depend only on its initial mass and the EOS. We thus have *almost* all the ingredients needed to determine the EOS, with the exception that the initial mass of the NS is not known. In the following, we show how one can constrain the EOS using these observations and the observed distribution of NS masses in binary NS systems [33–35]. We also show how the EOS constraints will improve given a gravitational wave (GW) measurement of the binary inspiral (i.e., prior to coalescence) with Advanced LIGO and Virgo.

We focus on the observations presented in Rowlinson et al. [5], in which X-ray plateaus were observed following initial SGRB triggers using *Swift*. The light curves fit the prediction of a protomagnetar that is being spun-down through dipole electromagnetic radiation [11] (as noted in Rowlinson et al. [5], this is consistent with the late-time residual spin-down phase being driven by a relativistic magnetar wind [36]), allowing the authors to obtain p_0 and B_p from the model.

Rowlinson et al. [5] present data for a number of ob-

TABLE I: The short γ-ray burst (SGRB) sample containing central engines used in this article, with all data and fits from Ref. [5]. z, p_0, B_p and $t_{\rm col}$ are respectively the redshift, initial spin period, surface dipolar magnetic field and collapse time. The bottom four SGRBs do not collapse within 10^4 – 10^5 s.

GRB	z	p_0 [ms]	B_p [10^{15} G]	$t_{\rm col}$ [s]
060801	1.13	$1.95^{+0.15}_{-0.13}$	$11.24^{+1.93}_{-1.78}$	326
070724A	0.46	$1.80^{+1.04}_{-0.38}$	$28.72^{+1.42}_{-1.29}$	90
080905A	0.122	$9.80^{+0.78}_{-0.77}$	$39.26^{+10.24}_{-12.16}$	274
101219A	0.718	$0.95^{+0.05}_{-0.05}$	$2.81^{+0.47}_{-0.39}$	138
051221A	0.55	$7.79^{+0.31}_{-0.28}$	$1.80^{+0.14}_{-0.13}$	–
070809	0.219	$5.54^{+0.48}_{-0.43}$	$2.06^{+0.48}_{-0.42}$	–
090426[a]	2.6	$1.89^{+0.08}_{-0.07}$	$4.88^{+0.88}_{-0.90}$	–
090510	0.9	$1.86^{+0.04}_{-0.03}$	$5.06^{+0.27}_{-0.23}$	–

[a]Duration ($T90$=1.2s) suggests GRB090426 is a SGRB, however its host and prompt characteristics remain ambiguous [e.g. 37, 38].

jects with accurate redshift measurements. As this is required to determine the rest-frame light curve, and hence p_0 and B_p, we omit any SGRBs for which the redshift is not known. We are left with four SGRBs that collapse and four that are long-term stable[1], which are presented in Table I.

The values of B_p and p_0 are derived assuming electromagnetic dipolar spin-down, with perfect efficiency in the conversion between rotational energy and electromagnetic radiation. We discuss the possibility of a lower efficiency below. Note that a mass of $1.4M_\odot$ and radius of 10 km were also assumed, although the dependence on these parameters is weak [4, 5]. The standard spin-down formula is [39]

$$p(t) = p_0 \left(1 + \frac{4\pi^2}{3c^2}\frac{B_p R^6}{I p_0^2} t\right)^{1/2}, \qquad (1)$$

where R and I are the radius and moment of interia respectively of the NS. For a given EOS, one can write the maximum gravitational mass, $M_{\rm max}$, as a function of the star's rotational kinetic energy [39, 40], and hence p. For slow rotation

$$M_{\rm max} = M_{\rm TOV}\left(1 + \alpha p^\beta\right), \qquad (2)$$

where, in Newtonian gravity $\beta = -2$ and α is a function of the star's mass, radius and moment of inertia. We evaluate equation (2) in relativistic gravity by creating equilibrium sequences of $M_{\rm max}(p)$ using the general relativistic hydrostatic equilibrium code `RNS` [41]. We then calculate a functional fit to these equilibrium sequences to get α and β for each EOS.

A supramassive protomagnetar collapses when the star's period becomes large enough that $M_{\rm p} = M_{\rm max}(p)$, where $M_{\rm p}$ is the mass of the protomagnetar. The collapse time, $t_{\rm col}$, is found by substituting (1) into (2) with $t = t_{\rm col}$ and $M_{\rm max} = M_{\rm p}$. Solving for $t_{\rm col}$ gives

$$t_{\rm col} = \frac{3c^3 I}{4\pi^2 B_p^2 R^6}\left[\left(\frac{M_{\rm TOV} - M_{\rm p}}{\alpha\, M_{\rm TOV}}\right)^{-2/\beta} - p_0^2\right]. \qquad (3)$$

Equation (3) gives the time for a supramassive protomagnetar to collapse to a black hole given observed parameters (p_0, B_p, $M_{\rm p}$) and parameters related to the EOS ($M_{\rm TOV}$, R and I). Note that equation (3) does not account for several effects, such as how I and B_p change with time as the star spins down, or how the presence of matter outside the star affects the spindown torque, a point we discuss below.

The observations in Ref. [5] give B_p, p_0 and $t_{\rm col}$, implying we require $M_{\rm p}$ in equation (3) to constrain the EOS. We obtain $M_{\rm p}$ statistically from the observed masses of NSs in binary NS systems [33–35], where the most up-to-date measurements give $M = 1.32^{+0.11}_{-0.11}\,M_\odot$, with the errors being the 68% posterior predictive intervals [35]. Numerical simulations of binary NS mergers and observations of SGRBs indicate that $\lesssim 0.01\,M_\odot$ of material is ejected during the merger [e.g., 24, 42, and references therein]. Modulo this lost mass, which we ignore in the following, it is the rest mass of a system that is conserved through the merger. An approximate conversion between gravitational and rest masses is $M_{\rm rest} = M + 0.075M^2$ [43], which leads to a gravitational mass for the protomagnetar following an SGRB merger of $M_{\rm p} = 2.46^{+0.13}_{-0.15}\,M_\odot$.

In Figure 1 we plot the collapse time, $t_{\rm col}$, as a function of the protomagnetar mass, $M_{\rm p}$, for each of the SGRBs listed in Table I. We utilise five EOSs that are consistent with current observations and have a range of maximum masses: SLy [44] ($M_{\rm TOV} = 2.05\,M_\odot$, $R = 9.97$ km; black curve), APR [45] ($2.20\,M_\odot$, 10.00 km; orange), GM1 [46] ($2.37\,M_\odot$, 12.05 km; red), AB-N [47] ($2.67\,M_\odot$, 12.90 km; green) and AB-L [47] ($2.71\,M_\odot$, 13.70 km; blue).

Consider GRB 060801 in Figure 1, with B_p and p_0 given in Table I. EOS GM1 (red curves) requires $M_{\rm p} \approx 2.38\,M_\odot$ for it to collapse 326 s following the initial burst. On the other hand, EOS SLy (black curves) requires $M_{\rm p} \approx 2.06\,M_\odot$, which falls well outside the 2σ posterior mass distribution. The quoted errors for B_p and p_0 have little effect on this result. Similarly, GRB 101219A requires $M_{\rm p} \approx 3.00 M_\odot$ for AB-L and $M_{\rm p} \approx 2.82\,M_\odot$ for AB-N, which both lie at the extreme high-mass end of the distribution. In this sense, all of the GRBs plotted in the two left-hand columns of Figure 1 favour the inter-

[1] There were six SGRBs that are long-term stable and satisfy our criteria, however two of these (GRBs 050509B and 061201) did not show conclusive fits to the magnetar model, and were therefore labelled by Ref. [5] as 'possible candidates'. We omit these in the present analysis, although note that they are consistent with our general conclusions.

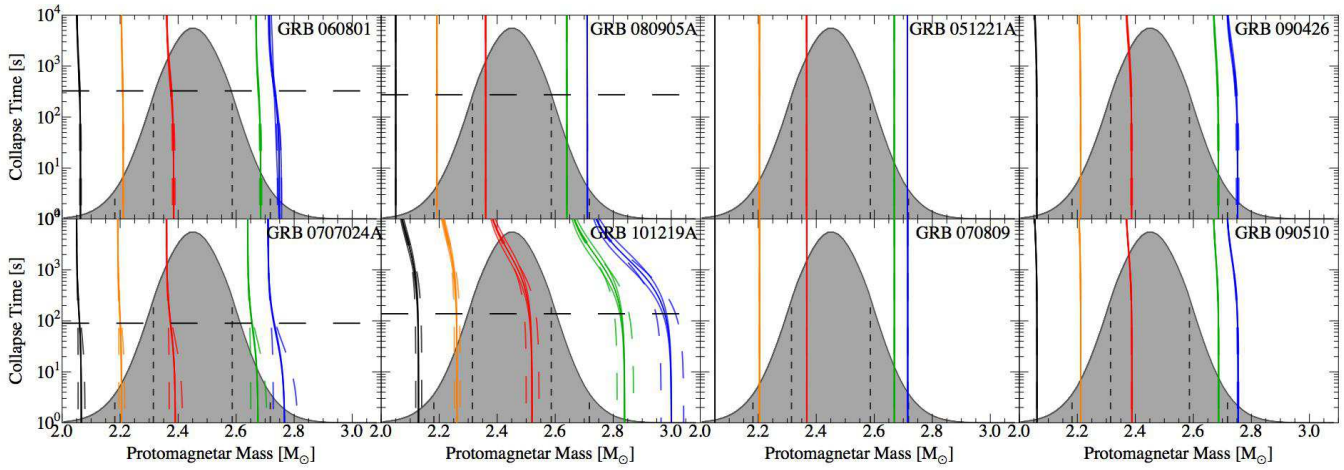

FIG. 1: Collapse time as a function of the protomagnetar mass for each of the SGRBs in Table I. The two left-hand columns are those in which the protomagnetar collapses to form a black hole, where the collapse time is given by the horizontal dashed black line. The two right-hand columns are those SGRBs that form stable protomagnetars. The theoretical collapse time for each equation of state is calculated from equation (3), where the initial spin period and magnetic field distributions are given in Table I for each GRB. Five EO are shown in each panel: SLy (black), APR (orange), GM1 (red), AB-N (green) and AB-L (blue). The dark solid curve for each equation of state assumes the values of p_0 and B_p given in Table I with the 68% confidence intervals in p_0 and B_p included in the faded dashed and faded solid curves respectively. The shaded region is the protomagnetar mass distribution that results from merging two neutron stars whose masses are independently drawn from the binary neutron star mass distribution of Ref. [35], with the 68% and 95% mass intervals represented with the vertical dashed lines.

mediate EOSs. It is worth noting that the EOSs we plot are a representative sample that cover a wide range of maximum masses; many more EOSs fit into the intermediate regime that would be satisfied by the constraints we are placing herein. For an up-to-date review of plausible EOSs see Ref. [32].

It is worth paying special attention to GRB 080905A. Rowlinson et al. [5] found relatively large p_0, implying slow spin down from electromagnetic torques. In the 274 s before GRB 080905A collapses, the protomagnetar has spun down from $p_0 = 9.8$ ms to between $p = 10.2$ ms and $p = 10.9$ ms depending on the EOS. For any EOS, this requires a fine-tuning in the protomagnetar mass. There are many interpretations for this fine-tuning. Fan et al. [48] proposed that this is evidence that the protomagnetar was predominantly spun down through GW losses as opposed to electromagnetic torques. This is possible, although we note that the ellipticity of the star needs to be $\sim 10^{-2}$–10^{-3}, which requires an average internal toroidal field of almost 10^{17} G for a star with $M \gtrsim 2.5\,M_\odot$ [49]. On the other hand, the isotropic efficiency of turning rotational energy into electromagnetic energy is assumed to be 100%. Reducing the assumed efficiency or beam opening angle also leads to a reduction of the initial spin period. Other possibilities include a chance alignment that led to a false host-galaxy identification, or ongoing accretion or propellering that is affecting the pulsar spin down [50]. It is clear that these are crucial issues that will have to be dealt with in a more systematic study if our method is to be used to obtain a strong, quantitative, constraint on the EOS.

The two right-hand columns of figure 1 are those SGRBs that are not observed to collapse. Their relatively high initial spin periods and low surface magnetic field strengths imply that they do not spin down significantly in ~ 100–1000 s. Therefore, as with GRB 080905A, each EOS curve is almost a vertical line. If $M_{\rm p} \leq M_{\rm TOV}$, these objects are stable magnetars, and will never collapse from loss of centrifugal support. On the other hand, they may still have $M_{\rm p} \gtrsim M_{\rm TOV}$, in which case they are unstable with $t_{\rm col} \gg 10^5$ s. If the latter is true, these GRBs could be candidate "blitzars" [51] that are a proposed physical mechanism behind fast radio bursts [FRBs; 52, 53]. In principal, if the blitzar model is correct one could utilise the method described herein to also constrain the EOS using FRBs, although a method for determining $t_{\rm col}$ would be required. A method for testing the blitzar model, in particular the connection between FRBs and GRBs, has recently been described in Ref. [54].

Figure 1 shows what currently can be achieved given that the mass of the GRB remnant can only be statistically inferred from binary NS observations. In the near future, Advanced LIGO and Virgo will begin measuring GWs from binary NS inspirals at a rate of 0.4 to 400 per year [55]. Importantly for our purposes, these instruments will measure the chirp mass, $\mathcal{M} = (m_1 m_2)^{3/5}/(m_1 + m_2)^{-1/5}$, and the symmetric mass ratio $\eta = (m_1 m_2)/(m_1 + m_2)^2$, where $m_{1,2}$ are the masses

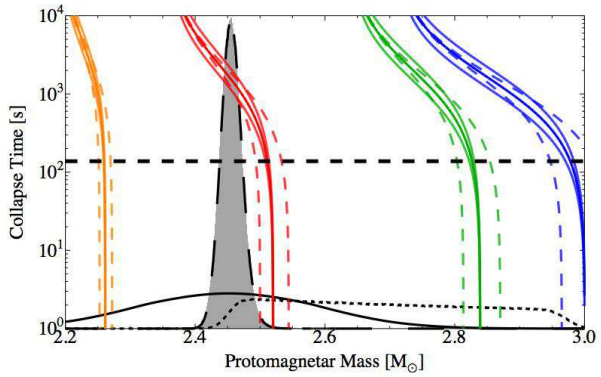

FIG. 2: Collapse time as a function of the protomagnetar mass for GRB 101219A. The five equations of state are described in the caption of Figure 1. The three protomagnetar mass distributions represent the binary neutron star mass distribution only (solid black; same as the distribution shown in Figure 1), the posterior mass distribution from a conservative Advanced LIGO/Virgo measurement of the progenitor chirp mass and symmetric mass ratio (dotted black) and the posterior mass distribution from the binary neutron star distribution and the conservative Advanced LIGO/Virgo progenitor measurement (dashed black with shading).

of the original progenitor NSs. The fractional 95% confidence intervals for these quantities will, at worst, be $\sim 2\%$ for $\mathcal{M}$ and $\sim 20\%$ for η [see 56, for details]. These measurements will allow m_1 and m_2 to be estimated. In Figure 2 we again plot the collapse time as a function of protomagnetar mass for GRB 101219A, but assume a hypothetical GW measurement of the merger of two $1.32\,M_\odot$ NSs with the aforementioned confidence intervals for $\mathcal{M}$ and η.

Figure 2 clearly shows that a combined measurement of the NS progenitor masses using GWs and knowledge of the prior NS mass distribution significantly tightens the constraints on the EOS. For example, assuming the GM1 EOS (red curve in Figure 2) implies a protomagnetar mass for the remnant of GRB 101219A of $M_{\rm p} = 2.51^{+0.02}_{-0.02}\,M_\odot$ (68% confidence interval). While this is broadly consistent with the expectation of $M_{\rm p} = 2.45^{+0.14}_{-0.14}\,M_\odot$ from current constraints on the binary NS mass distribution (see figure 1), this would be inconsistent with a putative Advanced LIGO measurement of $\mathcal{M}$ for the merger of two $1.32\,M_\odot$ NSs combined with binary NS mass distribution constraints. The latter would imply $M_{\rm p} = 2.46^{+0.02}_{-0.02}\,M_\odot$.

The apparent bias in the protomagnetar mass posterior distribution from Advanced LIGO-only measurements (dotted black curve of Figure 2) is caused by the bias in the estimation of η for some GW waveform templates [56]. Individual templates can, however, be used to estimate η with percent-level precision, which, when combined with measurements of $\mathcal{M}$, would render the binary NS mass distributions irrelevant in constraining protomagnetar masses.

How often does one expect a coincident GW and electromagnetic detection of an SGRB with an X-ray plateau? Using a conservative beaming angle of 8° [19, 57, and references therein] and the *Swift* sample of SGRBs corrected for dominant selection biases [58], we obtain an intrinsic rate of $820\,{\rm Gpc}^{-3}\,{\rm s}^{-1}$. With a binary NS horizon distance for coincident Advanced LIGO and Virgo detections [55, 59], and assuming 50% of all SGRBs have X-ray plateaus [5], we get a rate of 0.2 coincident electromagnetic and GW detections per year. The Space-based multi-band astronomical Variable Object Monitor (SVOM) has a decrease in sensitivity of a factor ~ 2 compared to *Swift*, but the higher triggering energy band may be more optimal for the detection of spectrally harder SGRBs. Assuming these two effects cancel, the increased sky coverage of SVOM over *Swift* implies ~ 0.4 coincident events per year. Finally, ISS-Lobster, a proposed all-sky X-ray imaging telescope, has been estimated to see about 2 coincident SGRBs per year [60], corresponding to about 1 per year with X-ray plateaus.

In this paper we have shown how one can constrain the nuclear equation of state from observations of short γ-ray bursts that exhibit X-ray plateaus. We have outlined how current understanding of the mass distribution in neutron star binaries can already be used to place constraints on the equation of state of dense matter and how a future coincident detection of a gravitational wave and X-ray signal from a binary neutron star merger could place significantly stronger constraints. This is an exciting prospect and the rates we have estimated for coincident detection suggest it is a very real possibility.

Given this encouraging starting point, it is crucial for future work to build on the method presented here and address in a more systematic way the caveats we have mentioned above (e.g., more detailed torque modelling, more accurate fits to light curves). This has the potential to allow for strong and truly quantitative constraints to be placed on the equation of state of dense matter.

ACKNOWLEDGMENTS

We are extremely grateful to Antonia Rowlinson for valuable comments about the manuscript. We also gratefully acknowledge Jordan Camp who carefully read the manuscript as part of a LIGO Scientific Collaboration review (LIGO document number P1300195). PDL is supported by the Australian Research Council (ARC) Discovery Project (DP110103347) and an internal University of Melbourne Early Career Researcher grant. EJH acknowledges support from a UWA Research Fellowship. DMC is supported by an ARC Future Fellowship and BH by an ARC DECRA Fellowship. VR is a recipient of a John Stocker Postgraduate Scholarship from the Science and Industry Endowment Fund. This work was made

possible through a UWA Research Collaboration Award.

* Electronic address: paul.lasky@unimelb.edu.au
† CSIRO Astronomy and Space Science, Australia Telescope National Facility, P.O. Box 76, Epping, NSW 1710, Australia

[1] P. T. O'Brien et al., Astrophys. J. **647**, 1213 (2006).
[2] J. A. Nousek et al., Astrophys. J. **642**, 389 (2006).
[3] P. A. Evans et al., Mon. Not. R. Astron. Soc. **397**, 1177 (2009).
[4] A. Rowlinson et al., Mon. Not. R. Astron. Soc. **409**, 531 (2010).
[5] A. Rowlinson, P. T. O'Brien, B. D. Metzger, N. R. Tanvir, and A. J. Levan, Mon. Not. R. Astron. Soc. **430**, 1061 (2013).
[6] B. P. Gompertz, P. T. O'Brien, G. A. Wynn, and A. Rowlinson, Mon. Not. R. Astron. Soc. **431**, 1745 (2013).
[7] B. Zhang, Y. Z. Fan, J. Dyks, S. Kobayashi, P. Mészáros, D. N. Burrows, J. A. Nousek, and N. Gehrels, Astrophys. J. **642**, 354 (2006).
[8] B. D. Metzger, E. Quataert, and T. A. Thompson, Mon. Not. R. Astron. Soc. **385**, 1455 (2008).
[9] Z. G. Dai and T. Lu, Astron. Astrophys. **333**, L87 (1998).
[10] Z. G. Dai and T. Lu, Phys. Rev. Lett. **81**, 4301 (1998).
[11] B. Zhang and P. Mészáros, Astrophys. J. L. **552**, L35 (2001).
[12] W.-H. Gao and Y.-Z. Fan, Chin. J. Astron. Astrophys. **6**, 513 (2006).
[13] D. Eichler, M. Livio, T. Piran, and D. N. Schramm, Nature **340**, 126 (1989).
[14] S. D. Barthelmy et al., Nature **438**, 994 (2005).
[15] E. Berger et al., Nature **438**, 988 (2005).
[16] J. S. Bloom et al., Astrophys. J. **638**, 354 (2006).
[17] M. D. Duez, Class. Quantum Grav. **27**, 114002 (2010).
[18] L. Rezzolla, B. Giacomazzo, L. Baiotti, J. Granot, C. Kouveliotou, and M. A. Aloy, Astrophys. J. Lett. **732**, L6 (2011), 1101.4298.
[19] N. R. Tanvir, A. J. Levan, A. S. Fruchter, J. Hjorth, R. A. Hounsell, K. Wiersema, and R. L. Tunnicliffe, Nature (London) **500**, 547 (2013), 1306.4971.
[20] E. Troja et al., Astrophys. J. **665**, 599 (2007).
[21] N. Lyons, P. T. O'Brien, B. Zhang, R. Willingale, E. Troja, and R. L. C. Starling, Mon. Not. R. Astron. Soc. **402**, 705 (2010).
[22] S. Dall'Osso, G. Stratta, D. Guetta, S. Covino, G. De Cesare, and L. Stella, Astron. Astrophys. **526**, A121 (2011).
[23] M. G. Bernardini, R. Margutti, J. Mao, E. Zaninoni, and G. Chincarini, Astron. Astrophys. **539**, A3 (2012).
[24] K. Hotokezaka, K. Kiuchi, K. Kyutoku, T. Muranushi, Y.-i. Sekiguchi, M. Shibata, and K. Taniguchi (2013), arXiv:1307.5888.
[25] T. W. Baumgarte, S. L. Shapiro, and M. Shibata, Astrophys. J. L. **528**, L29 (2000).
[26] S. L. Shapiro, Astrophys. J. **544**, 397 (2000).
[27] S. Rosswog and M. B. Davies, Mon. Not. R. Astron. Soc. **334**, 481 (2002).
[28] B. Giacomazzo and R. Perna, Astrophys. J. **771**, L26 (2013).
[29] G. B. Cook, S. L. Shapiro, and S. A. Teukolsky, Astrophys. J. **424**, 823 (1994).
[30] P. B. Demorest, T. Pennucci, S. M. Ransom, M. S. E. Roberts, and J. W. T. Hessels, Nature **467**, 1081 (2010).
[31] J. Antoniadis et al., Science **340**, 448 (2013).
[32] K. Hebeler, J. M. Lattimer, C. J. Pethick, and A. Schwenk, Astrophys. J. **773**, 11 (2013).
[33] B. Kiziltan, A. Kottas, and S. E. Thorsett, ArXiv e-prints (2010), 1011.4291.
[34] R. Valentim, E. Rangel, and J. E. Horvath, Mon. Not. R. Astron. Soc. **414**, 1427 (2011).
[35] B. Kiziltan, A. Kottas, M. De Yoreo, and S. E. Thorsett (2013), arXiv:1309.6635.
[36] B. D. Metzger, D. Giannios, T. A. Thompson, N. Bucciantini, and E. Quataert, Mon. Not. R. Astron. Soc. **413**, 2031 (2011).
[37] H.-J. Lü, E.-W. Liang, B.-B. Zhang, and B. Zhang, Astrophys. J. **725**, 1965 (2010).
[38] A. Nicuesa Guelbenzu, S. Klose, A. Rossi, D. A. Kann, T. Krühler, J. Greiner, A. Rau, F. Olivares E., P. M. J. Afonso, R. Filgas, et al., Astron. Astrophys. **531**, L6 (2011).
[39] S. L. Shapiro and S. A. Teukolsky, *Black holes, white dwarfs, and neutron stars: The physics of compact objects* (1983).
[40] N. D. Lyford, T. W. Baumgarte, and S. L. Shapiro, Astrophys. J. **583**, 410 (2003).
[41] N. Stergioulas and J. L. Friedman, Astrophys. J. **444**, 306 (1995).
[42] B. Giacomazzo, R. Perna, L. Rezzolla, E. Troja, and D. Lazzati, Astrophys. J. L. **762**, L18 (2013).
[43] F. X. Timmes, S. E. Woosley, and T. A. Weaver, Astrophys. J. **457**, 834 (1996).
[44] F. Douchin and P. Haensel, Astron. Astrophys. **380**, 151 (2001).
[45] A. Akmal, V. R. Pandharipande, and D. G. Ravenhall, Phys. Rev. C **58**, 1804 (1998).
[46] N. K. Glendenning and S. A. Moszkowski, Phys. Rev. Lett. **67**, 2414 (1991).
[47] W. D. Arnett and R. L. Bowers, Astrophys. J. S. **33**, 415 (1977).
[48] Y.-Z. Fan, X.-F. Wu, and D.-M. Wei, Phys. Rev. D **88**, 067304 (2013).
[49] B. Haskell, L. Samuelsson, K. Glampedakis, and N. Andersson, Mon. Not. R. Astron. Soc. **385**, 531 (2008).
[50] A. Rowlinson, Private Communication (2013).
[51] H. Falcke and L. Rezzolla (2013), arXiv:1307.1409.
[52] D. R. Lorimer, M. Bailes, M. A. McLaughlin, D. J. Narkevic, and F. Crawford, Science **318**, 777 (2007).
[53] D. Thornton et al., Science **341**, 53 (2013).
[54] B. Zhang (2013), arXiv:1310.4893.
[55] J. Abadie et al., Class. Q. Grav. **27**, 173001 (2010).
[56] J. Aasi et al., Phys. Rev. D **88**, 062001 (2013).
[57] I. Bartos, P. Brady, and S. Márka, Classical and Quantum Gravity **30**, 123001 (2013), 1212.2289.
[58] D. M. Coward, E. J. Howell, T. Piran, G. Stratta, M. Branchesi, O. Bromberg, B. Gendre, R. R. Burman, and D. Guetta, Mon. Not. R. Astron. Soc. **425**, 2668 (2012).
[59] LIGO Scientific Collaboration, Virgo Collaboration, J. Aasi, et al. (2013), arXiv:1304.0670.
[60] J. Camp, S. Barthelmy, L. Blackburn, K. G. Carpenter, N. Gehrels, J. Kanner, F. E. Marshall, J. L. Racusin, and T. Sakamoto, Experimental Astronomy (2013).